THERMOCHEMICAL MODELING AND CHEMICAL VAPOR DEPOSITION OF TWO-PHASE BORIDES IN THE Hf-Si-B-Cl-H SYSTEM

by

Eric Joseph Wuchina

Dissertation submitted to the Faculty of the

Virginia Polytechnic Institute and State University

in partial fulfillment of the requirements for the degree of

DOCTOR OF PHILOSOPHY

in

Materials Engineering Science

APPROVED:

Dr. Jesse J. Brown, Jr.
Chairman

Dr. Ronald S. Gordon

Dr. Ronald G. Kander

Dr. William T. Reynolds

Dr. Stephen Kampe

Dr. Inna G. Talmy

June 8, 1995
Blacksburg, Virginia

THERMOCHEMICAL MODELING AND CHEMICAL VAPOR DEPOSITION OF TWO-PHASE BORIDES IN THE Hf-Si-B-Cl-H SYSTEM

by
Eric Joseph Wuchina
Dr. Jesse J. Brown, Jr, Chairman
Department of Materials Engineering Science
(ABSTRACT)

Advanced, very high temperature materials that are ablation-resistant in oxidizing atmospheres are needed to withstand the severe environments found in rocket engine and aerospace vehicle applications. Boride-based coatings that form a protective layer during oxidation have been found to withstand these extreme conditions. Chemical vapor deposition has been chosen as a viable processing technique for producing these coatings. It is expected that two-phase boride coatings will have enhanced oxidation resistance over the single-phase materials by forming an oxide/glass layer to seal the base material from direct attack. Thermochemical modeling of CVD reactions was done to predict the processing conditions for the deposition of two-phase HfB_2-SiB_6 or HfB_2-SiB_4 coatings. The SOLGASMIX-PV computer program was used for these calculations, which were based on $ZrCl_4$, $SiCl_4$ BCl_3, and H_2 reactant gases. An array of temperatures (1100, 1300, and 1500K), total pressures (0.02, 0.1, and 1 atm.) and excess hydrogen concentrations (10:1, 25:1, and 50:1 H:(Zr + Si + B + Cl)) were investigated. These calculations show that two-phase HfB_2-SiB_6 and HfB_2-SiB_3 coatings are possible over a wide range of processing conditions, suggesting that a wide variety of two-phase compositions with a diverse

population of microstructures can be deposited. This points to the possibility of optimizing oxidation resistance of these coatings by varying the processing conditions. A hot-wall CVD reactor was designed and constructed specifically for deposition reactions in this system. It was found to be necessary to separately deliver $SiCl_4$ and BCl_3 to the hot zone to prevent reactions between them and to eliminate interference with the in-situ hafnium chlorination reaction. SiB_4, rather than SiB_6, was the preferred deposition product in the Si-B-Cl-H system. HfB_2 was the only compound found to deposit in the Hf-B-Cl-H system. Both borides coatings exhibited several different surface morphologies. The separate delivery of BCl_3 and $SiCl_4$, while necessary to prevent their gas phase reaction, caused reactant concentration gradients at the substrate surface due to poor mixing. This resulted in a variation of microstructural features across the substrate surface (both domed and faceted morphologies were deposited at the same temperatures), suggesting that reactant supersaturation is more important in determining surface morphology than temperature, pressure, and hydrogen concentration at the conditions studied. The first successful deposition of the two-phase HfB_2-SiB_4 coating was accomplished. Analysis of these two-phase coatings again reveals a broad range of microstructural characteristics, and the compositional gradients across the substrate surface also suggest the need for better gas mixing.

ACKNOWLEDGEMENTS

The author would like to thank the following:

- My parents, whose patience, love, guidance, and encouragement have made me a better person.

- My brother and sister, for always supporting me.

- Dr. and Mrs Jesse Brown, for helping spark my interest in research and my pursuit of a graduate education, as well as being good friends.

- Dr. Inna Talmy, for being my friend, mentor and avid supporter.

- Rick Lowden, for patiently answering my incessant questions. Our invaluable discussions have made much of this research possible.

- Bill, Robbie, Flynn, Heidi, Stephanie, and the other professional tailgaters for helping me recapture my school spirit, and making me remember why Tech is such a great place - its the people.

- Dr. Ron Kander, for encouraging a camaraderie among the students and fostering student-faculty interactions at the weekly "Fluid-Flow and Aerodynamics" Seminars.

- Drs. Bill Reynolds and Steve Kampe for valuable scientific discussions.

- Dr. Ronald Gordon, for teaching me valuable lessons that needed to be learned.

- Dr. Jim Zaykoski, for helping edit this manuscript and being a good friend.

- Dave Graham, for patiently teaching me the intricacies of SOLGASMIX.

- Dr. Bob Brizzolara, for assisting with the scanning electron microscopy.

- Drs. Mark Opeka and Bill Messick for supporting this research through the NSWC Materials Technology Program.

- Justin Cooper, for assisting with the x-ray calibration curve.

- Drs. James Sheehan and Robert Shinavski, for their advice on CVD reactions.

- The whole Fest crew, for remaining my friends for a long, long time.

- The staff at the High Temperature Materials Lab Users Facility, ORNL, for their assistance with the electron microprobe analysis.

- Susan Fleming and Lee Ann Ellis for helping to make my scheduled visits to campus less stressful.

TABLE OF CONTENTS

LIST OF TABLES....vii

LIST OF FIGURES....viii

CHAPTER 1. INTRODUCTION....1

CHAPTER 2. LITERATURE REVIEW

2.1 Boride Materials for Oxidation Resistance....3
2.2 Properties of SiB_4 and HfB_2....8
2.3 Phase Equilibria in the Hf-Si-B System....10
2.4 Chemical Vapor Deposition....15
2.4.1 Reaction Types....15
2.4.2 CVD Systems....18
2.4.3 Other Coating Technologies....20
2.4.4 Advantages and Disadvantages....22
2.4.5 Applications....23
2.4.6 Non-Coating Applications....26
2.5 CVD of Two-Phase Coatings....32
2.6 CVD of HfB_2 and SiB_4....36

CHAPTER III. RESULTS AND DISCUSSION....39

3.1. Thermodynamic Modeling of CVD Reactions....39

3.1.1 Results of Modeling Reactions in the Zr-Si-B-Cl-H System....39
3.1.2 Discussion of Thermodynamic Modeling Results....49
A. Calculation Technique Used for Modeling....49
B. Discussion of Modeling Zr-Si-B-Cl-H System....52
C. The Role of Thermodynamics in CVD....55

3.2 Reactor Design....63

3.2.1 Hot-Wall vs. Cold-Wall Systems....63
3.2.2 Reactor Design....66
3.2.3 Gas Delivery System....68
$SiCl_4$ Flowrate Calibration....72
3.2.4 Pressure Control and Exhaust System....78

3.3 Source Materials....81

3.4 Experimental Procedure....82

3.5. Characterization....85

3.6 Deposition and Characterization of CVD Coatings....86

3.6.1 SiB_4....87
3.6.2 HfB_2....97
3.6.3 HfB_2-SiB_4....103

3.7 Discussion of CVD Results....132

3.7.1 Kinetics and Mass Transport Issues during CVD....132
3.7.2 Microstructural Development - Nucleation and Growth of Films..129
3.7.3 Uniformity and Adherence of CVD Coatings....154
3.7.4 Deposition Results....157

3.8 SUMMARY....162

3.9 CONCLUSIONS....163

APPENDIX A....165

REFERENCES....191

VITA....200

LIST OF TABLES

Table 1. Oxidation Behavior of HfC and HfB_2 in 7% Oxygen as a Function Temperature and Time[2]

Table 2. The Properties of HfB_2 and SiB_4

Table 3. Thermodynamic Properties of Gaseous Species Used in SOLGASMIX Calculations

Table 4. Thermodynamic Properties of Condensed Species Used in SOLGASMIX Calculations

Table 5. Properties of Hf and Zr[78]

Table 6. Experimental Conditions for SiB_4 Deposition

Table 7. Experimental Conditions for HfB_2 Deposition

Table 8. Experimental Conditions for Two-Phase HfB_2-SiB_4 Deposition

LIST OF FIGURES

Figure 1. Thermogravimetric Analysis of CrB_2, CrB_2/Al_2O_3, and $CrB_2/Al_2O_3/SiB_4$ Ceramics[7]

Figure 2. The Si-B System[23]

Figure 3. The Hf-B System[27]

Figure 4. The Hf-Si System[26]

Figure 5. The Hf-Si-B System at 1300°C[28]

Figure 6. Schematic of Forced Flow, Thermal Gradient Chemical Vapor Infiltration of Preform for Producing Ceramic Matrix Composites[35]

Figure 7. Scanning Electron Micrograph of Si_3N_4 Deposited on SiC Fibers at Hot Face[35]

Figure 8. Scanning Electron Micrograph of Cross Section of Composite Produced by CVI[35]

Figure 9. Output from SOLGASMIX Computer Program at 1100K and 0.01 atm.

Figure 10. Ternary CVD Phase Diagram at P = 1 atm., T = 1300K, and H/(Zr + Si + B + Cl) = 10

Figure 11. Binary CVD Phase Diagram at $X_{ZrCl4} = 5\%$

Figure 12. Schematic Diagram Illustrating Sequentially-Linked Steps in a CVD Process[84]

Figure 13. Original Design for the Hot-Wall CVD Reactor

Figure 14. $SiCl_4$ Bubbler

Figure 15. Calibration Curve of $SiCl_4$ Flowrate vs. H_2 Flowrate

Figure 16. Final Design of Hot-Wall CVD Reactor

Figure 17. Schematic of Complete Chemical Vapor Deposition System

Figure 18. Scanning Electron Micrographs of Fibrous Coating on Graphite

Figure 19. X-Ray Diffractogram of SiB_4 Coating on Graphite

Figure 20. Scanning Electron Micrographs of SiB_4 Coating Showing Domed Morphology

Figure 21. Scanning Electron Micrographs of SiB_4 Coating Showing Preferred Growth of Some Grains

Figure 22. Scanning Electron Micrographs of SiB_4 Coating Showing Faceted Morphology

Figure 23. X-Ray Diffractogram of HfB_2 Coating on Graphite

Figure 24. Scanning Electron Micrographs of HfB_2 Coating Showing Porous Coating with Spherical Morphology

Figure 25. Scanning Electron Micrographs of HfB_2 Coating Showing Domed Morphology

Figure 26. Scanning Electron Micrographs of HfB_2 Coating Showing Faceted Morphology

Figure 27. X-Ray Diffractograms of HfB_2-SiB_4 Powder Mixtures for Quantitative Analysis

Figure 28. X-Ray Calibration Curve

Figure 29. X-Ray Diffractogram of HfB_2-SiB_4 Two-Phase Coating on Graphite

Figure 30. Scanning Electron Micrographs of HfB_2-SiB_4 Coating Showing a) Separate Faceted Crystals, b) Crystals Inpinging Upon One Another, c, d) Continuous Dense Coating

Figure 31. Scanning Electron Micrographs of HfB_2-SiB_4 Coating Showing a) Discontinuous and b) Continuous Domed Grains

Figure 32. Scanning Electron Micrographs of HfB_2-SiB_4 Coating Showing Preferred Grain Growth

Figure 33. Scanning Electron Micrographs of HfB_2-SiB_4 Coating Showing Development of Clusters of Preferred Growth Grains

Figure 34. Scanning Electron Micrographs of HfB_2-SiB_4 Coating Showing a) Spherical, and b) Platelet Morphology

Figure 35. Scanning Electron Micrographs of HfB_2-SiB_4 Coating Showing Development of Second-Phase Clusters

Figure 36. Scanning Electron Micrographs of HfB_2-SiB_4 Coating Showing Faceted and Domed Morphologies, Along with Branched Clusters

Figure 37. Scanning Electron Micrographs of HfB_2-SiB_4 Coating Showing Clusters Growing from Faceted Grains

Figure 38. Scanning Electron Micrographs of HfB_2-SiB_4 Coating Showing a) Dark and Light Colored Surface and b) Transition Region at Higher Magnification

Figure 39. Scanning Electron Micrographs of HfB_2-SiB_4 Coating Showing Development of Darker Phase

Figure 40. a) Scanning Electron Micrograph Image, b) Hf x-ray map, and c) Si x-ray map of HfB_2-SiB_4 Coating

Figure 41. Scanning Electron Micrographs of HfB_2-SiB_4 Coating Showing Coexistance of Faceted SiB_4 and Domed HfB_2 Morphologies

Figure 42. Backscattered Electron Image of Faceted Crystal on Domed Primary Coating, from HfB_2-SiB_4 Coating

Figure 43. Scanning Electron Micrographs of HfB_2-SiB_4 Coating Showing Two Different Morphologies

Figure 44. Scanning Electron Micrographs of HfB_2-SiB_4 Coating Showing Coexistence of Two Different Morphologies

Figure 45. a) Scanning Electron Micrograph, b) Hf X-Ray Map, and c) Si X-Ray Map of HfB_2-SiB_4 Coating Showing That Small White Crystals are HfB_2 and Continuous Dark Phase is SiB_4

Figure 46. Backscattered Electron Image of HfB_2-SiB_4 Coating Showing Two Different-Sized Faceted Crystals on the Domed Primary Phase

Figure 47. a),b) Scanning Electron Micrographs and, c) Si X-Ray Map of HfB_2-SiB_4 Coating Showing Faceted Second Phase on Domed Continuous Phase

Figure 48. a) Scanning Electron Micrograph, b) Backscattered Electron Image, and c) Si X-Ray Map of HfB_2-SiB_4 Coating Showing Highly Faceted Second Phase on a Domed Continuous Phase

Figure 49. Typical Temperature Dependence of Deposition Rate

Figure 50. Typical Flow Rate Dependence on Deposition Rate[104]

Figure 51. The Basic Modes of Film Growth[31]

Figure 52. Scanning Electron Micrographs Showing Development of Morphology of SiC Films[106]

Figure 53. Effect of Processing Conditions on Microstructure[32]

Figure 54. Schematic Representation of Coating Microstructures Deposited by CVD a) Columnar Grains with Domed Tops; b) Faceted, Columnar Grains; and c) Equiaxed Grains[34]

Figure 55. The Evolution of Columnar Microstructures During CVD[107]

Figure 56. The Integration of Descrete Particles into the Growing Film[108]

Figure 57. Hook-Shaped Whisker Formed by Repetitive Change in Growth Direction[109]

Figure 58. Scanning Electron Micrographs of Textured Surfaces Deposited by CVD[111]

CHAPTER 1. INTRODUCTION

1.1 Background

The borides of the group IV-VII transition metals display a number of unique properties, including high melting point, very high hardness and strength, high thermal conductivity and relatively low thermal expansion, as well as high chemical stability. This combination of properties make borides potential candidates for various structural applications requiring high temperature strength, thermal stress resistance, and stability in severe environments (especially oxidizing atmospheres). Borides can have application as protective coatings, cutting tools, armor shielding, and electrodes for aluminum smelting. In particular, boride-based materials are being considered as excellent candidates for high-temperature ablation-resistant components (such as nosetips and leading edges) on advanced aerospace vehicles.

The goal of this research is to produce two-phase HfB_2-SiB_4 composite coatings. It is expected that this coating will have enhanced oxidation resistance over the end-member boride materials. Since it is anticipated that the necessary material properties do not need to be exhibited by the bulk material structure, a surface coating can be applied to achieve the desired performance characteristics for the given application. Chemical vapor deposition has been chosen as the processing route for making these

materials due to the ability to control compound stoichiometry, chemical purity, coating morphology, orientation, and crystal structure. (Additionally, the use of this material as a matrix in composites processed by chemical vapor infiltration can be a goal.)

This dissertation will thus seek to give the reader a proper background for the proposed research. The Introduction (Section I) will include a review of CVD processing, a summary of boride material development, the properties HfB_2 and SiB_4 ceramics, previous CVD studies of these compounds, the known phase equilibria in the Hf-Si-B system, the two-phase materials that have been deposited by CVD, thermodynamics and kinetics issures in CVD, and a discussion of the coating microstructures that can be produced by CVD. The thermochemical modeling of reactions in the Zr-Si-B-Cl-H system using the SOLGASMIX computer program will be described, with a discussion of the relevance of the approach, in the Section II. The design and construction of a hot-wall CVD reactor specifically for the preparation of two-phase coatings in this chemical system and the experimental procedure will be covered in Section III. The results, discussion, and conclusions are given in Section IV.

CHAPTER 2. LITERATURE REVIEW

2.1 Boride Materials for Oxidation Resistance

Advanced, very high temperature materials that are ablation-resistant in oxidizing environments are needed to withstand the rapid heating and cooling environments found in rocket engine and aerodynamic vehicle applications. The sharp edges needed for maneuverability, as well as the temperatures and stresses endured during these missions make current carbon ablators and silicon-based ceramics unsuitable for advanced applications. The ability to withstand high heating rates to 2760°C, plus long exposure times at lower temperatures, coupled with near zero recession rates are the target materials selection criteria for re-entry and engine applications. NASA, NSWC, and the Air Force all have programs aimed at advanced materials development. Several materials research programs are focused on either the modification of known baseline materials or creating novel compounds or composites for these applications.

Silicon-based ceramics are excellent in oxidizing environments at temperatures up to 1500°C due to the formation of a passive, self-healing SiO_2 layer. At higher temperatures or reduced pressures, the formation of SiO gas (active oxidation) causes rapid material loss and ultimately, component failure.

The driving force for this research is to develop a material that will

oxidize at a slow rate to minimize the material recession. The performace criteria are based on the needs of a particular application, with the effects of exposure times, heating rates, oxygen pressures, and mechanical stresses all contributing to the selection of a particular material. At the temperatures, oxygen pressures, and stresses experienced during service, all materials will undergo some degree of oxidation, ablation, or melting. For most applications, the formation of an oxide layer is not necessarily detrimental to performance. The oxide needs to be able to withstand the surface stresses and temperatures while protecting the underlying structure.

Graphite and carbon/carbon composites use ablation techniques to dissipate the high heat fluxes generated during service, but the need for shape stability has precluded their use for some applications. Refractory carbides (non-silicon-based) have excellent high temperature oxidation resistance, but at lower temperatures, recession rates can be high due to the lack of a self-healing glass layer to protect the bulk structure.

The focus of recent studies of high-temperature oxidation-resistant materials has been based on an extensive program at ManLabs funded by the Air Force[1] in the 1960's. In this program, a variety of materials, including borides, carbides, silicides, graphites, and refractory metals were evaluated for high-temperature oxidation resistance, with HfB_2 and ZrB_2, emerging as the most versatile materials for a wide array of conditions. HfB_2

was found to form a thin oxide layer in plasma arc tests. A comparison of the oxidation behavior of HfC and HfB_2 over the temperature range 1500-2200°C for exposure times of 10 minutes to 10 hours is shown in Table I[2,3]. It is seen that HfB_2 performs much better than HfC at lower temperatures and shorter times.

Clougherty[4], Hinze[5] and Rasky[6] have reported that additions of up to 20% SiC to HfB_2 and ZrB_2 improved the oxidation resistance of the diborides due to the formation of a continuous glass layer. (HfB_2 and ZrB_2 both form adherent, high-melting temperature oxides, with HfB_2 slightly ouperforming ZrB_2. Both HfO_2 and ZrO_2 undergo phase transformations at high temperatures that might affect performance. Recent evidence suggests that since the HfO_2 goes through this transformation at higher temperatures, it happens closer to the outer surface, and doesn't affect oxide adherence.) Early stages of oxidation showed a parabolic rate dependence, suggesting that diffusion through the oxide layer is the rate controlling mechanism. Below 1100°C, a porous ZrO_2 scale forms, with B_2O_3 liquid filling the void space to protect the underlying structure from direct oxidation. Above 1100°C, boria vaporizes and at 1400°C, it is no longer protective. The SiC addition, at temperatures above 1200°C, helps to form a borosilicate glass that retards the vaporization of boria and acts as an effective barrier to oxygen diffusion. SiC is only slightly oxidized at 1300°C, with SiC particles

still embedded in the ZrO_2 and glass scale. The addition of other silicon-bearing compounds, such as Si_3N_4 or metal silicides were also found to improve oxidation performance. Recent work[7] has shown that different boride materials do not oxidize in the same manner; the formation of a continuous protective layer is system dependent. NbB_2 shows a slight weight loss at $T > 1100°C$, due to the concurrent formation of niobium oxide and evaporation of boria. CrB_2, on the other hand, shows a significant weight gain that levels out at 1100°C. The Cr_2O_3 and B_2O_3 react to form a continuous chromium borate ($CrBO_3$) film that acts as an effective diffusion barrier. The hot-pressed boride monoliths studied by the Air Force, however, were found to suffer from poor thermal shock resistance and low fracture toughness, and the emergence of SiC, Si_3N_4, and ceramic composites reduced interest in boride materials during the 1970's and 1980's.

The purpose of this research is to integrate recent knowledge with the results of previous researchers. The substitution of SiB_4 for SiC in the HfB_2-SiC composites should still provide increased oxidation resistance over pure HfB_2 by the formation of a borosilicate glass that seals the pores and cracks in the high-melting temperature HfO_2 that forms from the oxidation of HfB_2. This substitution is done to provide a simpler system for co-deposition, as the co-deposition of borides and carbides might be kinetically unfavorable, as described in Section 2.5.

Table 1. Oxidation Behavior of HfC and HfB_2 in 7% Oxygen as a Function Temperature and Time[2]

Temp. (°C)	HfC Oxide Thickness (μm)			HfB_2 Oxide Thickness (μm)		
	10 min	1 h	10 h	10 min	1 h	10 h
1500	96	236	746	6	15	47
1700	179	438	1,385	24	60	190
1800	233	571	1,804	114	684	6,840
1900	296	725	2,294	264	1,584	15,840
2100	451	1,104	3,491	1,200	7,200	72,000
2200	542	1,327	4,199	2,304	13,824	138,240

2.2 Properties of SiB_4 and HfB_2

The group IV diborides display a number of unique properties, including high melting point, very high hardness and strength, high thermal conductivity and relatively low thermal expansion, as well as high chemical stability. The high hardness and good thermal and electrical properties have made these materials useful in cutting tool, armor shielding, and electrode applications[8]. It is primarily the good oxidation behavior and high melting temperatures displayed by these materials that make them attractive for future aerospace applications. Some material properties of HfB_2 are listed in Table II[9]. The oxidation behavior of HfB_2 was reviewed in the previous section.

The existence of the silicon borides was first reported in the 1900's by Moisan and Stock[10]. A surge in interest in these materials during the early 1960's centered around the low specific gravity, oxidation, mechanical, and electrical behavior of these compounds to make lightweight structures and electronic devices. Several methods have been used to prepare pure SiB_4 ceramics. The reaction of the elements in air at elevated temperatures by Brewer[11] and Stavrolakis[12] was not successful, but later work by Colton[13] and Tremblay and Angers[14] utilized an argon atmosphere to produce the compound, with excess silicon or boron later etched away to leave pure SiB_4. Samsonov[15] used hot pressing of the elemental powders or a thermite

reaction between SiO_2 and B_2O_3 to produce the tetraboride.

Characterization of these materials has been reported by many of these researchers. X-ray diffraction studies by Brosset and Magnuson[16] and Matkovich[17] showed that this material has a rhombohedral crystal structure, with lattice parameters (and other properties) given in Table 2. Feigelson and Kingery[18] and Rizzo[19] describe the oxidation of SiB_4 in terms of the production of a thin borosilicate layer that is protective up to the decomposition temperature of 1400°C. Talmy, Zaykoski, and Wuchina[20] have found that the addition of SiB_4 to CrB_2-based ceramics have resulted in a dramatic improvement in the oxidation resistance, as shown in Figure 1.

Table 2. The Properties of HfB_2 and SiB_4

	HfB_2	SiB_4
Melting/Decomposition Temperature (°C)	3380	1400
Elastic Modulus (GPa)	500 (10% decrease above 1000°C)	300
Density (g/cm^3)	10.7	2.42
Hardness (kg/mm^2)	2900	2000
Crystal Structure	Hexagonal	Rhombohedral
Lattice Parameters (Å)	a = 3.15, c = 3.48	a = 6.33, c = 12.74
Thermal Expansion (x 10^6 mm/mm/K)	$\alpha_a = 5.21$ $\alpha_c = 6.03$	$\alpha_{bulk} = 5.8$

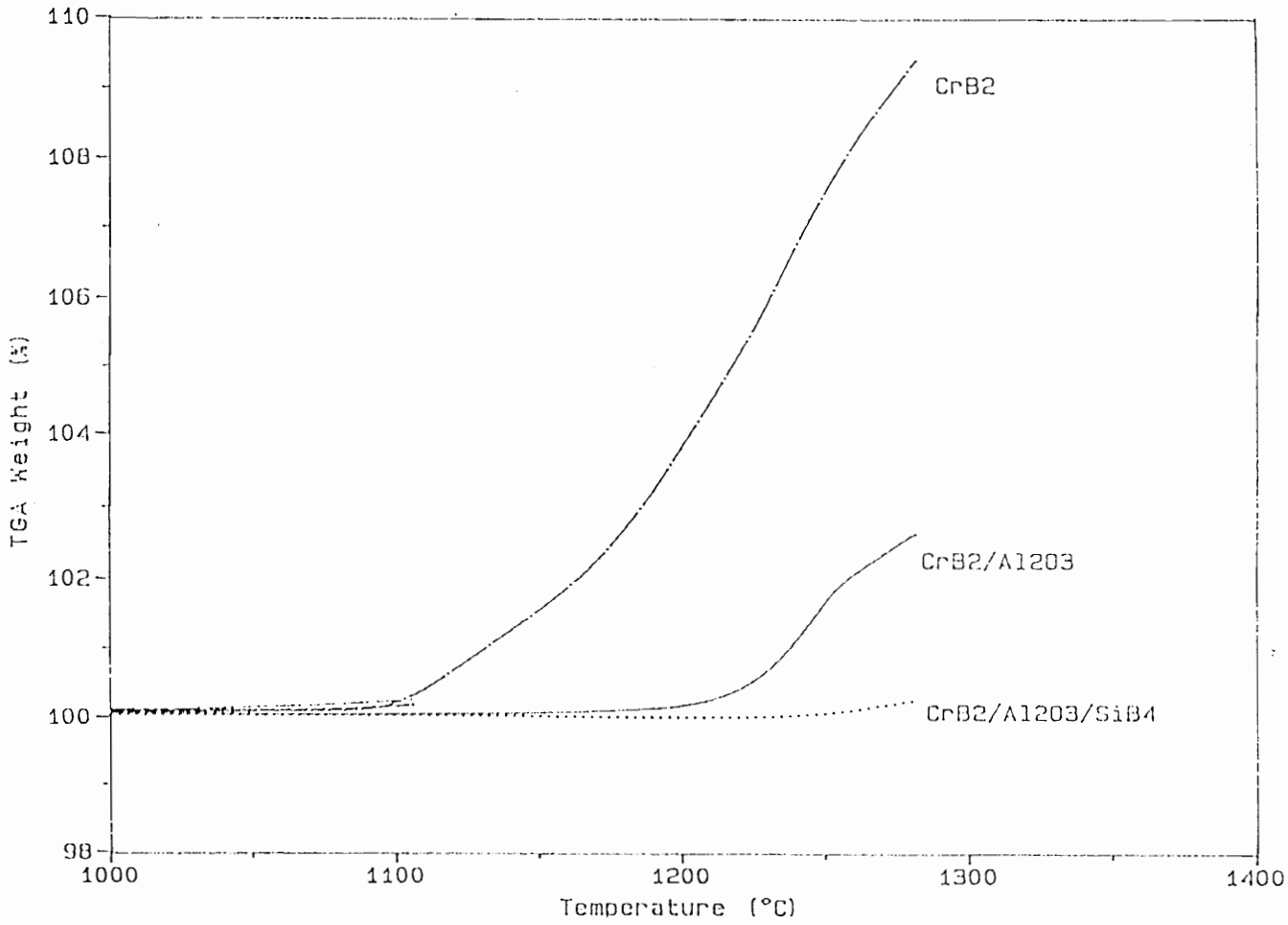

Figure 1. Thermogravimetric Analysis of CrB_2, CrB_2/Al_2O_3, and $CrB_2/Al_2O_3/SiB_4$ Ceramics[7]

2.3 Phase Equilibria in the Hf-Si-B System

i. The Si-B System

There have been a number of studies of compounds in the Si-B system. There has been some controversy regarding the composition of the lower boride phase. Early work by Moisan[10] identified this phase as SiB_3, while subsequent reports listed this phase as SiB_4 [13,16,17,19,21]. This lower boride has been reported to be a nonstoichiometric phase, SiB_n, with $n = 2.8$ to 5. Presently, it seems pretty well established that this phase is SiB_4, with the JCPDS Powder Diffraction Files[22] listing it as the tetraboride. The Si-B system contains two other stable compounds, SiB_6 and another non-stoichiometric compound, commonly given as SiB_{14}. The phase equilibrium diagram constructed by Olensinski and Abbaschian[23] shown in Figure 2 is generally accepted as the best representation of this system.

ii. The Hf-B System

Rudy and Windisch[24] first established the phase equilibrium (Shown in Figure 3) for the Hf-B system based on the work of a number of researchers. Two compounds, the high-melting temperature diboride (HfB_2) and monoboride (HfB) are reported. A complete review of the equilibria, phase stoichiometry, solubility, crystal chemistry, and thermodynamic data is given by Rogl and Potter[25].

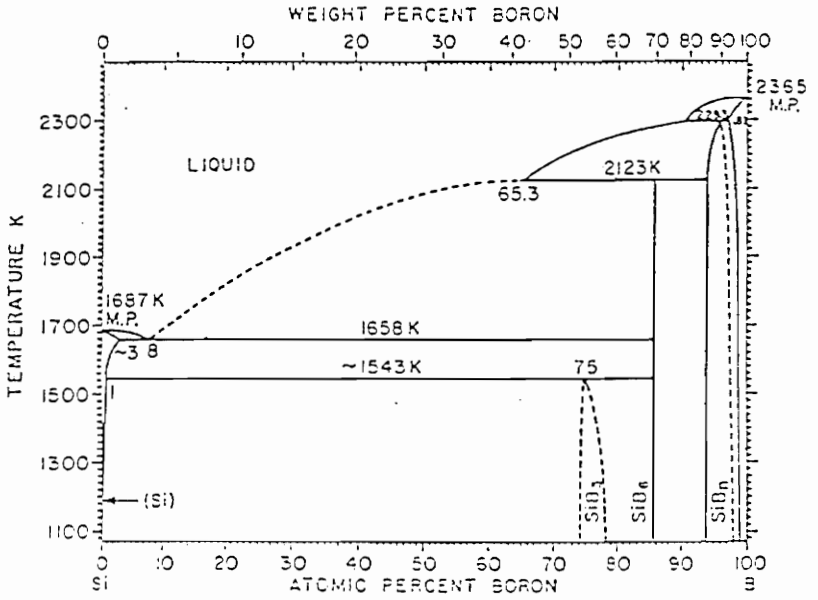

Figure 2. The Si-B System[23]

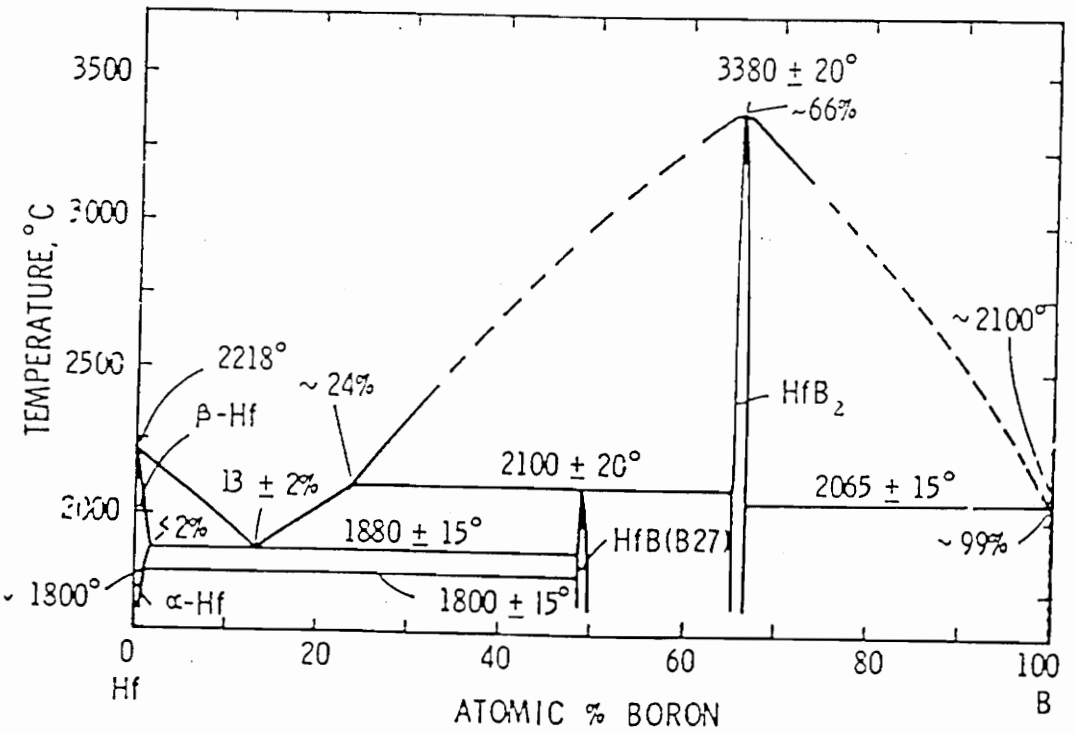

Figure 3. The Hf-B System[27]

iii. The Hf-Si System

Gokhale and Abbaschian[26] assessed the phase diagrams reported for the Hf-Si System, and concluded that the diagram of Brukl[27], shown in Figure 4, is most accurate. A discussion of the formation and melting temperatures, as well as crystal structure data for the five compounds in this system are given in this review. Thermodynamic data for these compounds have not been reported.

iv. The Hf-Si-B System

Rudy[28] published the 1300°C isothermal section for the Hf-Si-B system, as seen in Figure 5. This is the only known investigation of this ternary system. A ternary compound identified as a $D8_8$- Nowotny phase of composition $Hf_{52}Si_{38}B_{10}$ was reported.

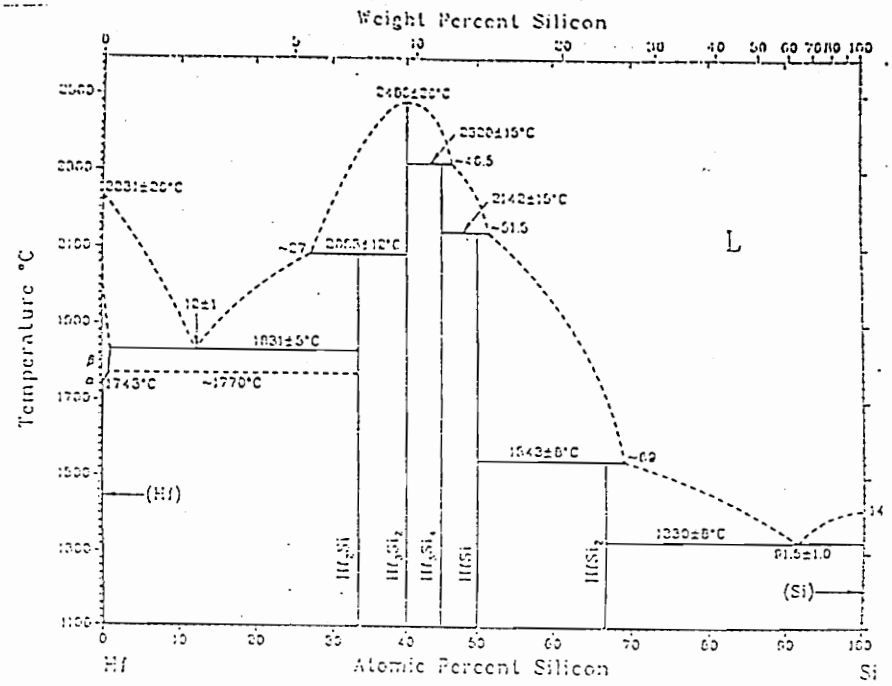

Figure 4. The Hf-Si System[26]

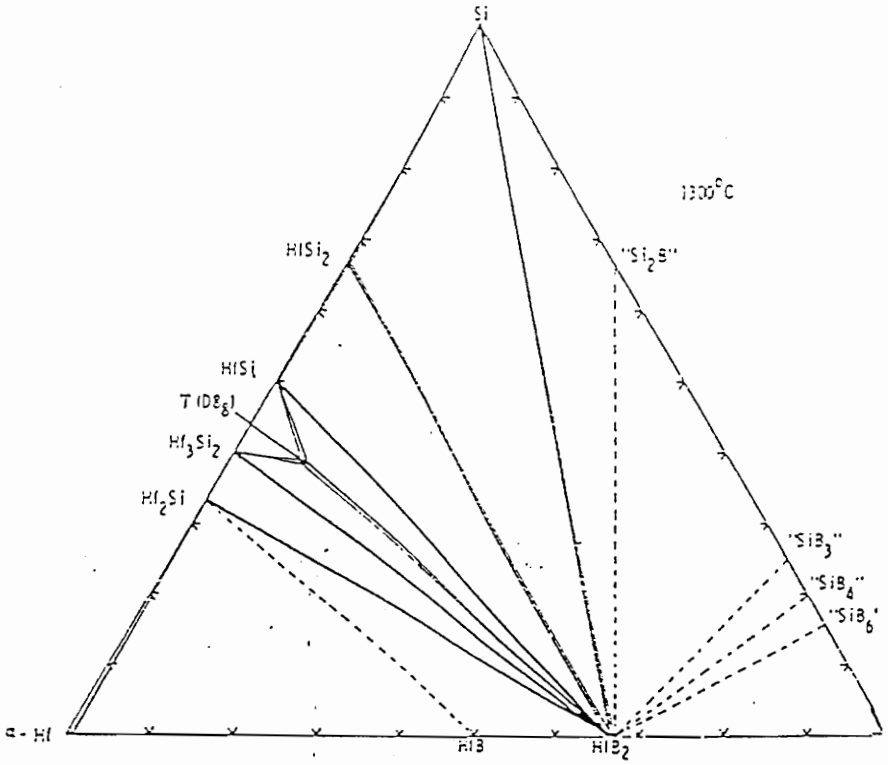

Figure 5. The Hf-Si-B System at 1300°C[28]

2.4 Review of Chemical Vapor Deposition

Chemical vapor deposition (CVD) is a process where gaseous precursors flow into a reactor, and chemical reactions take place to produce a solid coating on a substrate plus gaseous reaction products. In conventional CVD processes, the thermal energy supplied by the heated substrate drives the reaction, and product gases are removed from the reaction zone by fresh reactant gases continually supplied to the substrate.

CVD is not a new process. Its first practical use was in the 1880's, with tungsten deposits made by the hydrogen reduction of WF_6 being used to improve the strength of incandescent filaments. The iodine decomposition work of Van Arkel and deBoer[29] during the 1920's is commonly referred to as the origin of modern CVD technology. The production of high-purity refractory metals by the carbonyl (Mond) process was the other major pre-WWII use of CVD. The 1960's and 1970's brought the greatest advances in CVD technology, due to the development of semiconductor fabrication and the introduction of plasma and metal-organic technologies.

2.4.1 Reaction Types

The chemical reaction is the basic element of the CVD process. These deposition reactions can be classified into several general categories, all widely used in industrial production processes. These include: thermal